Heliyon 8 (2022) e09871

Contents lists available at ScienceDirect

Heliyon

journal homepage: www.cell.com/heliyon

Research article

Geometrical modelling of neuronal clustering and development

Ali H. Rafati [a,*], Maryam Ardalan [a,b,c], Regina T. Vontell [d], Carina Mallard [b], Gregers Wegener [a]

[a] Translational Neuropsychiatry Unit, Department of Clinical Medicine, Aarhus University, 8000 Aarhus C, Denmark
[b] Institute of Neuroscience and Physiology, Centre for Perinatal Medicine and Health, Sahlgrenska Academy, University of Gothenburg, Gothenburg, Sweden
[c] Center of Functionally Integrative Neuroscience-SKS, Department of Clinical Medicine, Aarhus University, Aarhus, Denmark
[d] Department of Neurology, University of Miami Miller, School of Medicine, Brain Endowment Bank, Miami, USA

ARTICLE INFO

Keywords:
Geometrical modelling
Mathematics
Neurites
Neuronal development
Neuronal shape
Neuronal-electrical field interaction
Vector field

ABSTRACT

The dynamic geometry of neuronal development is an essential concept in theoretical neuroscience. We aimed to design a mathematical model which outlines stepwise in an innovative form and designed to model neuronal development geometrically and modelling spatially the neuronal-electrical field interaction. We demonstrated flexibility in forming the cell and its nucleus to show neuronal growth from inside to outside that uses a fractal cylinder to generate neurons (pyramidal/sphere) in form of mathematically called 'surface of revolution'. Furthermore, we verified the effect of the adjacent neurons on a free branch from one-side, by modelling a 'normal vector surface' that represented a group of neurons. Our model also indicated how the geometrical shapes and clustering of the neurons can be transformed mathematically in the form of vector field that is equivalent to the neuronal electromagnetic activity/electric flux. We further simulated neuronal-electrical field interaction that was implemented spatially using Van der Pol oscillator and taking Laplacian vector field as it reflects biophysical mechanism of neuronal activity and geometrical change. In brief, our study would be considered a proper platform and inspiring modelling for next more complicated geometrical and electrical constructions.

1. Introduction

Neuronal connectivity and their distribution are pivotal for determining normal brain structural and functional development [1, 2]. The geometrical modelling of the neurons is a mathematically challenging issue but may help map details of neuronal shape differences seen in excitatory and inhibitory neurons [3, 4]. The neuronal geometry differs based on shape; either they can become pyramidal/spindle that are excitatory neurons while inhibitory neurons show more sphere-like shape [5]. The field could benefit from viewing how neurons form their connectivity and shape from a mathematical perspective, including broad neurite formation, overall neuronal shape formation, and parts of the neuronal development process. Understanding neuronal development in relation to excitatory and inhibitory synaptic plasticity seems unrealistic to implement a mathematical approximation model, and it is challenging to show reliable simulations. Therefore, characterising the pieces of this puzzle mathematically to provide a general algorithm [6] for approximate most of the process, would be very helpful in terms of Computational [7], Geometrical Learning and Cognitive neuroscience [4, 7]. The prerequisite for understanding brain function is to characterise the geometrical shape of cellular structure [8]. This approach would benefit understanding neural networks by building a *simulation* of the brain function based on the real geometrical shape [9]. Therefore, it will require considering how the brain chemical synapses work in multilayers [10, 11] and that needs to improve simulations in connection with geometrical characteristics of neurons that lead us to a stronger simulation of brain function. In this study, we have clarified at this step how geometrical shape of neurons in terms of neuronal-electrical interaction works in 3D as it is very important at biophysical scale [12].

Neuronal developmental modelling may generally be categorised into four steps: Part_1. Suggestive Mathematical Model of the Neural Branch Connectivity that models the complexity of neurites mathematically; Part_2. Suggestive Mathematical Model for Neuronal Shape and Development, provides a model for neuronal shape characterisation that can grow continuously to take the final shape of the neurons; Part_3. Assumed Model for Neuronal Clustering and its Vector Field to model a simple 3D_simulated neuronal clusters and neuronal electrical vector

* Corresponding author.
E-mail address: ali.h.rafati@clin.au.dk (A.H. Rafati).

https://doi.org/10.1016/j.heliyon.2022.e09871
Received 30 January 2022; Received in revised form 14 April 2022; Accepted 30 June 2022

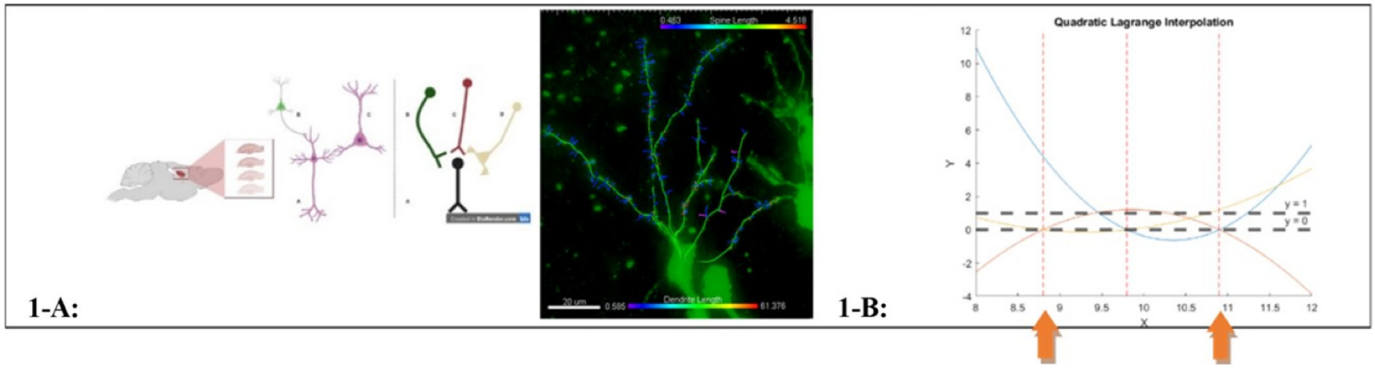

Fig. 1. Left, the schematic illustration of the neurons obtained from the hippocampus of mouse at the age of postnatal day (P) 12 indicates regular neuronal connections either straight or curved oriented between neurons. The 3D reconstructed basal neurons and neurites using Golgi staining are illustrated below. Right, there is a mathematical plot to investigate how neurites can orient theoretically based on the connection shown by Lagrange interpolation (1-B), two orange arrows indicate two points on position (X), indicating the ending with different connecting points on (Y) axis.

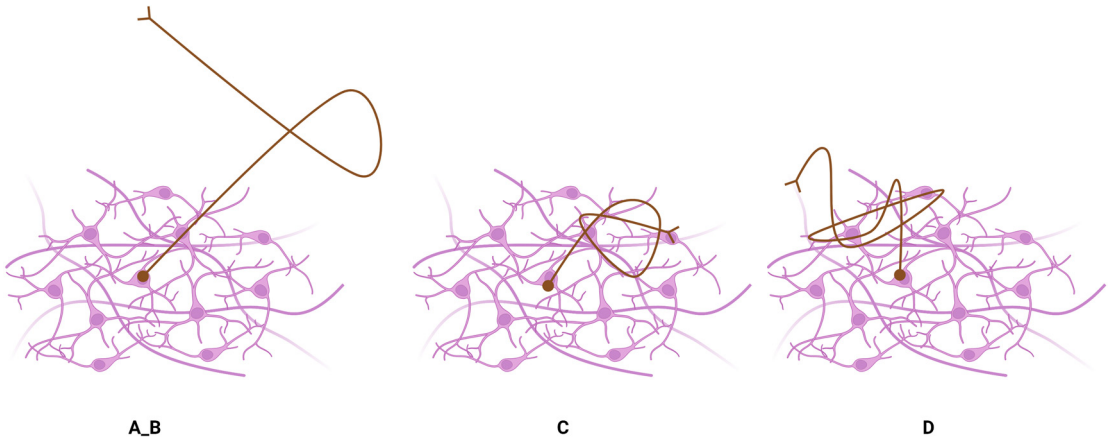

Fig. 2. Clarification of the idea of the "effect" of neighbouring neurons on one-side connected neurite (in Brown). In A, B, C and D, there are apparent changes in the shape and orientation of neurite, that either becomes convoluted C or distorted D, which depends on the type of calculation we use (see text).

field interaction; Part_4. Mathematical Model for Neuronal Organisation and Development, a mathematical model of 3D neuronal organisation and development. Here, we show how neurons, and their branches are complex and develop differently on a geometric scale according to the suggestive formula, for neuronal shape and growth modelling. Finally, we complement this discussion in detail using illustrations.

2. Results

2.1. The suggestive mathematical model of the neural branch connectivity

The distribution of neurons and their connectivity can be viewed from different angles. Here we aimed to clarify more about neurites spatial orientation followed by a mathematical model (see formula (1)–(2)). We hypothesised that generally, the distribution of neurites per se, either considering straight-line or curved-oriented form, can fit a model by Lagrange equation of a scalar function (the Lagrangian), Lagrange Interpolation Polynomial Fig. 1.B:

$$f(x) = p_n(x) = \sum_{k=0}^{n} \frac{l_k(x)}{l_k(x_k)} f_{(k)}; \tag{1}$$

$$l_k(x) = (x - x_0)(x - x_{k-1})(x - x_{k+1}) \ldots (x - x_n) \quad (0 < k < n) \tag{2}$$

Furthermore, to prove how they might develop naturally, we hypothesised that when the neurites typically stretch from the beginning of neuronal development, they make proper connections with adjacent neurons/cells. However, suppose the neurites are dissociated from the other side, growing like a free branch of a neuron. In that case, the neurites fail to develop and stretch naturally and may even be malformed substantially by showing retraction in a 3D geometric scale in the R^3, (see formula (3)–(9)), (Fig. 2, Fig. 3). We aimed to verify the 'effect' of the adjacent neurons on a free branch (tangent vector line) from one side, by modelling two components, a 'normal vector surface' that represented a group of neurons that for example, have electromagnetic/pressure 'effect' on a "neighbouring neurite" (tangent vector line) (Fig. 2, Fig. 3). We show the verification point in a schematic illustration Fig. 2, The mathematically equivalent plots are found in Fig. 3.

We measured the neuronal interaction by using the eigenvalues as the following formula was used in the first step to generate the 'Surface', which is indicated as "S" in the R^3:

$$S = \cos(X)\cos(Y) - \cos(X)\sin(Y); \quad -2\pi < X < 2\pi, \; X = Y \tag{3}$$

While to generate the 'Line' and the 'Tangent Vector line' (Fig. 3),

$$0.3 < r < 6; \quad 0 < t < 2\pi; \quad 0 < phi < 2\pi$$

$$X = r\cos(t)\sin(\phi) \tag{4}$$

$$Y = r\sin(\phi)\sin(t) \tag{5}$$

$$Z = r\cos(\phi) \tag{6}$$

In the next step, the vector field that is the direction of the normals on a surface was found and used eigenvalues of the surface; $Av = \lambda v$ and multiplied to X, Y, Z respectively. So, the line change is a function of the mentioned formula. That shows a substantial change in the line, and distorted "Blue Line" in comparison with "Red Line", Fig. 3.C.

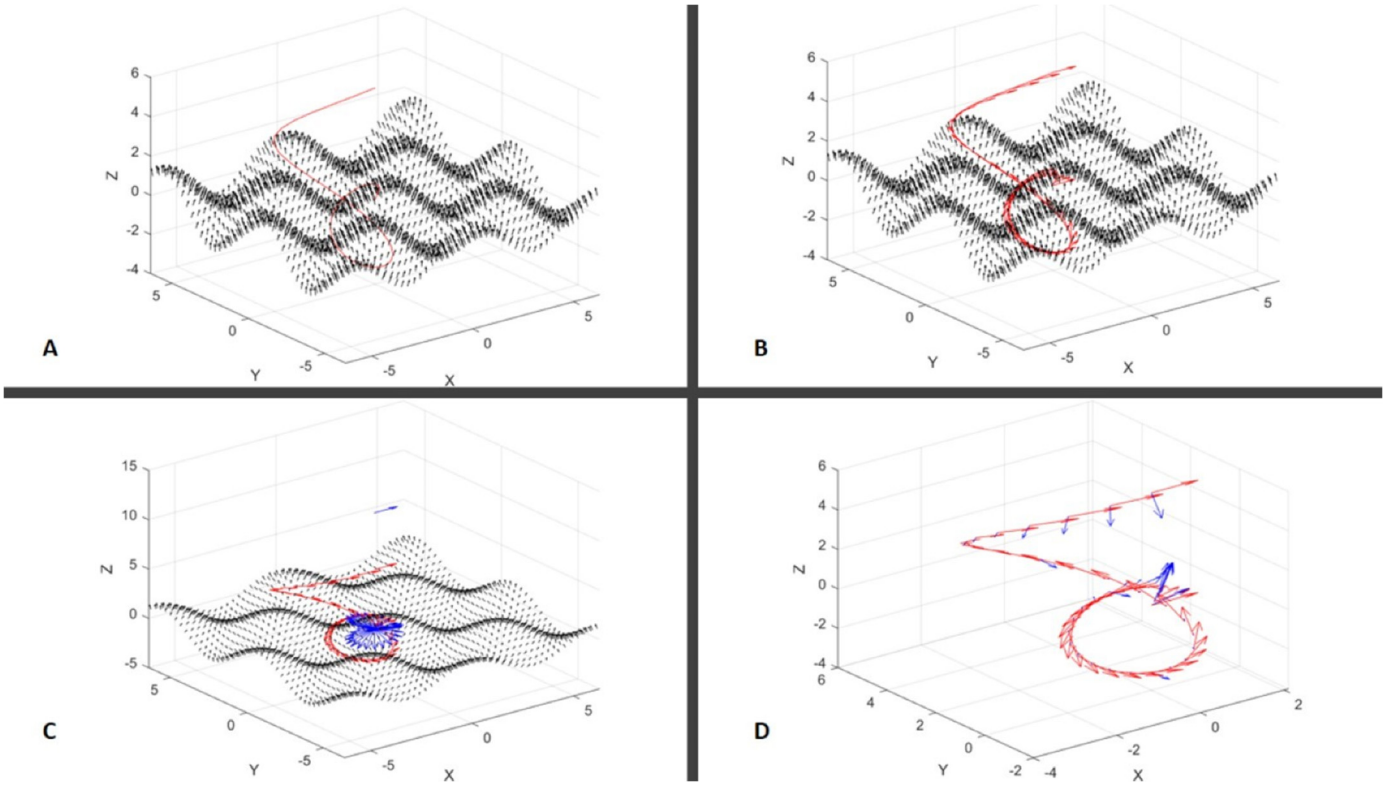

Fig. 3. The generated plots from A to D indicate the possible effect of neighbouring neurons (Black Normal Vector Surface) on the assumed spiral line, which represents neurite (Red Line and tangent Vector Line) in the R^3. The change in the shape of the line secondary to the normal surface vector field is detected like a Blue Line. Distortion in shape and orientation from one side is observable in C and D. The C and D were calculated differently. The surface in D is removed to show the red and blue lines clearly.

In addition, we used another mathematical equation, Fig. 3.D. and the equation $Av = \lambda v$ with the following parameters (formulas (7), (8), (9)), which included the first and second order partial differential equations arranged like "Jacobian matrix", and then solved by decomposition for V1, V2, V3 that reflects itself in Fig. 3.D like "Blue Vectors".

$$S' = \cos(Y)\sin(X) + \sin(X)\sin(Y); \quad -2\pi < X < 2\pi,\ X = Y \tag{7}$$

$$S'' = \cos(X)\cos(Y) - \cos(X)\sin(Y); \quad -2\pi < X < 2\pi,\ X = Y \tag{8}$$

$$\begin{bmatrix} X & \cdots & Z \\ \vdots & \ddots & \vdots \\ \frac{\partial^2 X}{\partial^2 r \partial^2 t \partial^2 \varphi} & \cdots & \frac{\partial^2 Z}{\partial^2 r \partial^2 t \partial^2 \varphi} \end{bmatrix} \begin{bmatrix} V1 \\ V2 \\ V3 \end{bmatrix} = \begin{bmatrix} \lambda 1 & 0 & 0 \\ 0 & \lambda 2 & 0 \\ 0 & 0 & \lambda 3 \end{bmatrix} \begin{bmatrix} S \\ \frac{\partial S}{\partial X \partial Y} \\ \frac{\partial^2 S}{\partial^2 X \partial^2 Y} \end{bmatrix} \tag{9}$$

Here, we postulated that the existence of a connected network of neurites before it begins to fully develop is a prerequisite for a normal neurite network development, otherwise based on our model, it appears that if the neurites grow with only one connected side, they became more spiral or even distorted than normally stretching and that will be resulted in abnormality in neuronal synaptic (excitatory/inhibitory) plasticity.

2.2. The suggestive mathematical model for neuronal shape and development

This part aimed to introduce a mathematical model that generates a cellular model that behaves naturally like a neuronal cell which means it can grow, changes in shape and take effects from its centre as a "nucleus" that is indeed a 'Fractal Cylinder', mathematically called 'surface of revolution' to generate the manifolds around the axis which is a 'Fractal Cylinder'. The schematic illustration of the geometrical changing of neurons is shown in Fig. 4. We generated corresponding mathematical models that follow these criteria summarised in Fig. 5 and Fig. 6.

Next, to generate a cell that can grow mathematically and change in shape, we made a 'Fractal Cylinder' that is transformable to a 3D object (formula (4)–(6)).

Next, we used the 'Riemann Zeta function' (formula (10));

$$\left\{\zeta(z) \quad \text{if} \quad 1 < \text{real}(z); \quad \sum_{k=1}^{\infty} \frac{1}{k^z}\right. \tag{10}$$

Then took the 'Taylor' (5^{th} order) (formula, (11)–(13)); If we use the following 'Taylor Expansion' of formulas (4), (5), (6) placed for 'z', then the formulas (11), (12), (13) are obtained, and the 'imaginary numbers' are ignored:

$$\mathrm{T(X)} = \frac{r\cos(s)t^5}{120} - \frac{r\cos(s)t^3}{6} + r\cos(s)t \tag{11}$$

$$\mathrm{T(Y)} = \frac{r\sin(s)t^5}{120} - \frac{r\sin(s)t^3}{6} + r\sin(s)t \tag{12}$$

$$\mathrm{T(Z)} = \frac{rt^4}{24} - \frac{rt^2}{2} = r \tag{13}$$

In the next step, we generated the "Cone" and the "Fractal Cylinder", if we generate a plot out of 'Taylor expansion' we get a simple "Cone" (see Fig. 5), however, if we apply the 'Riemann Zeta function' on them, then we obtain a "Fractal Cylinder" (see Fig. 5). Additionally, the whole shape and sizes are controllable simply by the value of 'r'.

Further, when we changed the 'Riemann Zeta function' applied 'Taylor expansion' in formulas (10)–(13) and converted them to formulas (14), (15), (16), the following plots were generated in Fig. 6. Plots showed that based on the value 'r', the shapes changed from "Fractal Cylinder" to "Pyramidal" or "Sphere-like" (Fig. 6: A, B). But in case applying the 'Riemann Zeta function' on the sphere formula *without* using 'Taylor expansion', we generated simply Fig. 6.D, which was based on the 'r' value. It also gave us the "Pyramidal Shape", with outpouching like neurites. The importance of this model is that in neurobiology, two

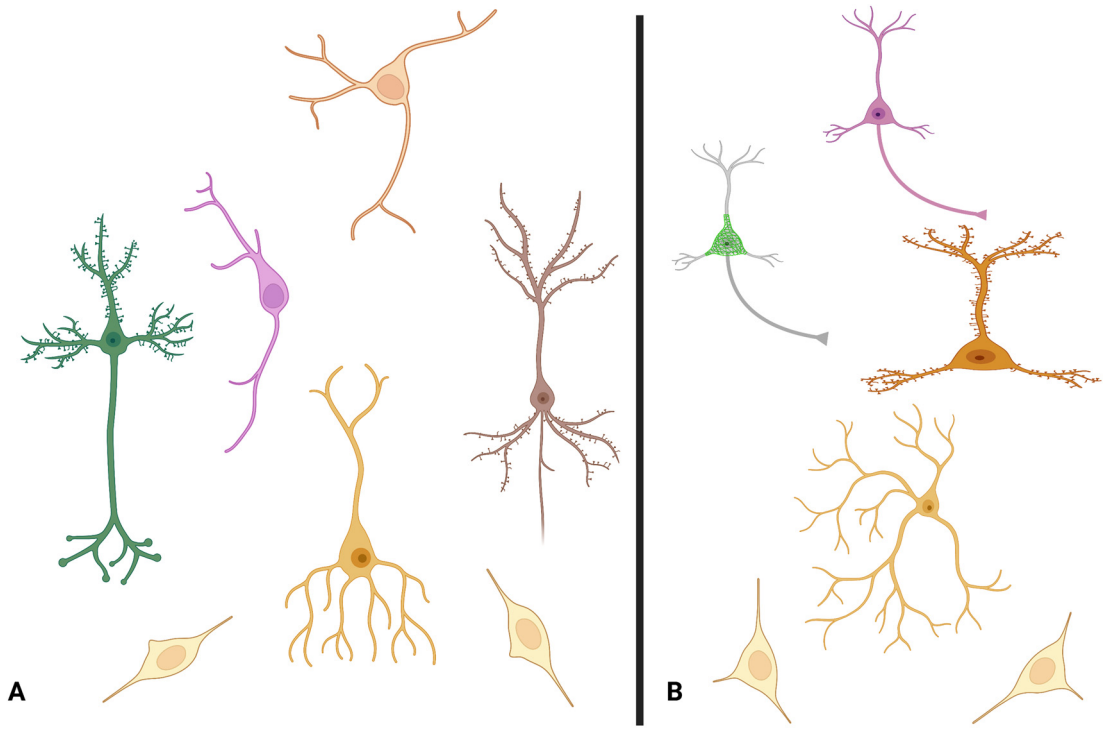

Fig. 4. The neuronal cells can change from neuronal progenitor cells to branched mature neurons. It represents the relation between shape and function. (A) The pyramidal and spindle cells originate from progenitor cells located at the bottom. (B) The progenitor cell on the right side differentiates to interneurons that looks more sphere-like.

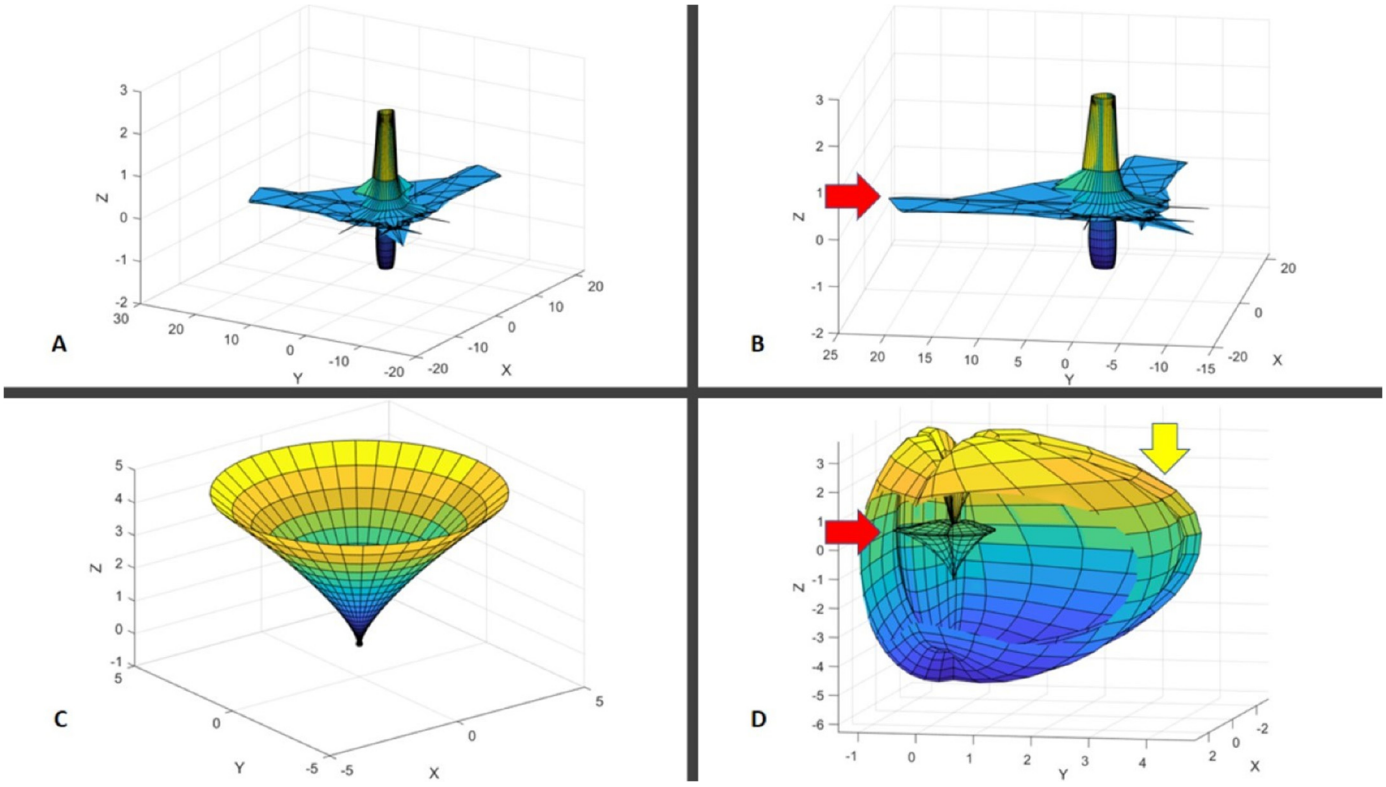

Fig. 5. Two series of plots are generated that bottom "Cone" is related to Taylor expansion while the top "Fractal cylinder "is related to applied Riemann Zeta function on the "Taylor expansions". As evident in 'D', the fractal cylinder is inside the generated figures shown in full views in Fig. 6.A to Fig. 6.C. In D, the sectioned cell is shown, the red arrow indicates the "Fractal Cylinder" that looks like a "Neuronal Nucleus" while the yellow arrow indicates the neuronal cell surface.

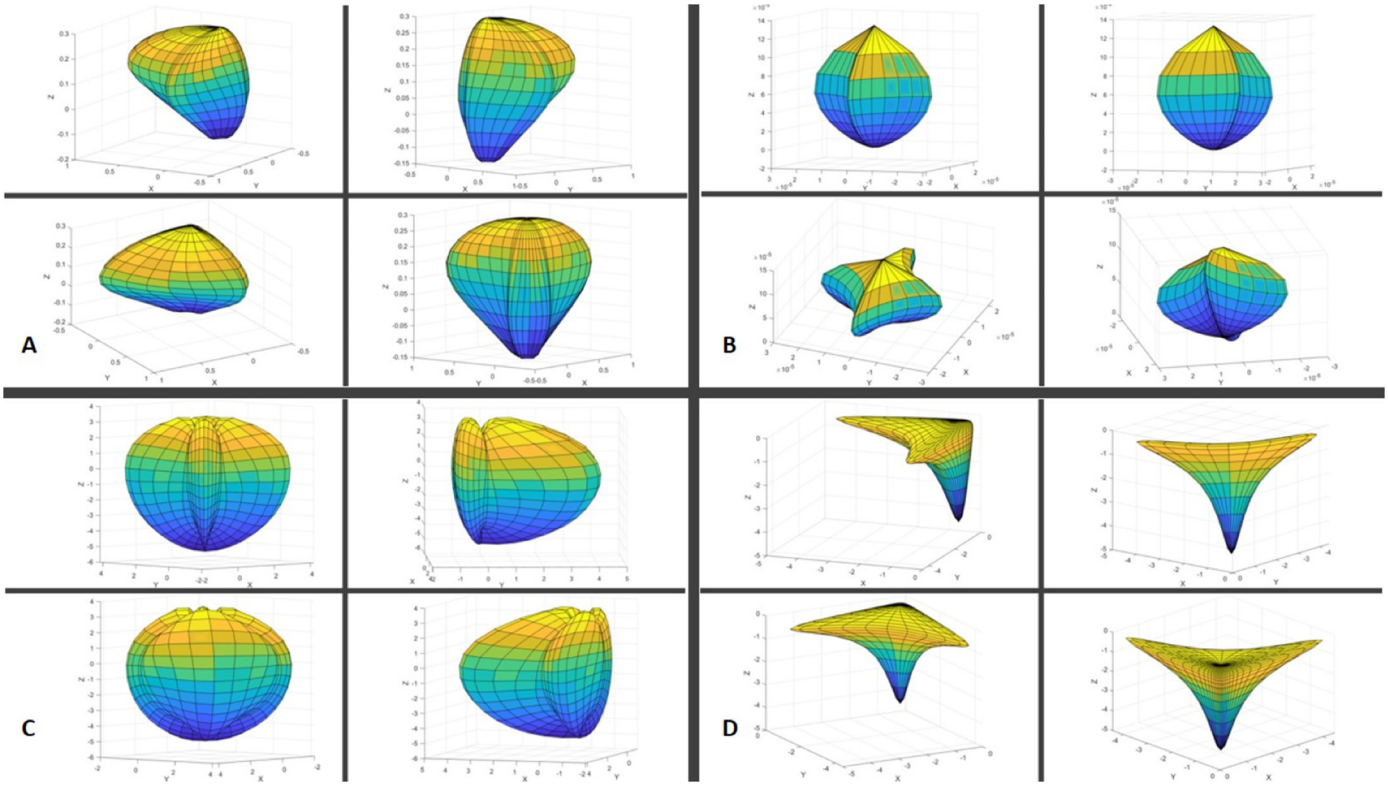

Fig. 6. The generated plots A to C are based on the "Fractal Cylinder" that acts like a "Nucleus" in cell to grow cells or change their shape from the centre to outward. This is comparable with D that doesn't contain the Cylinder but still shows some type of "branched pyramidal neuron". However, the "Sphere-like" figure in 'C' was generated with the "$r = -e^{\cos(p)^2 \sin(p)^2}$" and represented 'Sphere-like', non-pyramidal cells compared to Figures A, B, D that represents 'Pyramidal Neurons'.

different mathematical models may regulate independently, the "Cell Shape" and the "Neuronal branching patterns". In contrast, to generate the "Sphere-like neurons" that reflects the non-pyramidal, inhibitory neurons, we used 'r' value that was controlled by $r = -e^{\cos(p)^2 \sin(p)^2}$, $-2\pi < p < 2\pi$, Fig. 6.

$$Z(X) = \frac{r\cos(s)\sin(t)}{\left(\zeta\left(e^{\frac{r\cos(s)r^5}{120} - \frac{r\cos(s)r^3}{6} + r\cos(s)t}\right)^2\right)} \tag{14}$$

$$Z(Y) = \frac{r\sin(s)\sin(t)}{\left(\zeta\left(e^{\frac{r\sin(s)r^5}{120} - \frac{r\sin(s)r^3}{6} + r\sin(s)t}\right)^2\right)} \tag{15}$$

$$Z(Z) = \frac{r\cos(s)(t)}{\left(\zeta\left(e^{\frac{r^4}{24} - \frac{r^2}{2} + r}\right)^2\right)} \tag{16}$$

2.3. The assumed model for neuronal clustering and its vector field

This model represented as an example of a mathematically developed 3D model of neuronal clustering, Fig. 7. First, a schematic illustration in Fig. 7.A represented two ensembles of neurons (Fig. 7.A.1) which were projected on a plane Fig. 7.A.2.

Further, we showed in Fig. 7.B, an ensemble of neurons generated mathematically to mimic neuronal clustering in two rows. The next step was to explore the vector field of those neurons that may reflect their electromagnetic activity projected in 2D by using the gradient of on the differentiable manifolds for more details and for Laplacian vector field, see below [13] Fig. 7.C.

This model indicated how the geometrical shapes and clustering of the neurons can be transformed mathematically into the form of a vector field equivalent to the neuronal electromagnetic activity. The mathematical details are found below.

We used formula (4), (5), (6) that were replaced with the parameters $[x, y, z]$ in formula (17) to generate a symmetric surface orthogonal to z_axis, Fig. 7.B, however the gradient (formula (18)) of the same surface provided us with formulas (19), (20) and (21) that was seen as a vector field, (Fig. 7.C). Therefore, that made it possible to design and approximate the electric flux among the neurons.

$$F = x^2y^2ze^{-2x^2}e^{-2y^2}e^{-2z^2} - 1 \tag{17}$$

So, as we had $F\ (x, y, z)$, then the gradient was written as:

$$\nabla F = \frac{\partial F}{\partial x}\hat{\imath} + \frac{\partial F}{\partial y}\hat{J} + \frac{\partial F}{\partial z}\hat{k} \tag{18}$$

Then it came out depending on the parameters three equations of gradient (G) of F as below:

$$G(x) = 2xy^2ze^{-x^2-y^2-z^2}e^{-x^2}e^{-y^2}e^{-z^2} - 4x^3y^2ze^{-x^2-y^2-z^2}e^{-x^2}e^{-y^2}e^{-z^2} \tag{19}$$

$$G(y) = 2x^2yze^{-x^2-y^2-z^2}e^{-x^2}e^{-y^2}e^{-z^2} - 4x^2y^3ze^{-x^2-y^2-z^2}e^{-x^2}e^{-y^2}e^{-z^2} \tag{20}$$

$$G(z) = x^2y^2e^{-x^2-y^2-z^2}e^{-x^2}e^{-y^2}e^{-z^2} - 4x^2y^2z^2e^{-x^2-y^2-z^2}e^{-x^2}e^{-y^2}e^{-z^2} \tag{21}$$

Which was plotted in Fig. 7.C.

2.4. Neuronal-electrical field interaction

We expand this section to provide a better understanding of the cellular shapes and the relation with electrical field. We designed the following simulation that clarifies the effect of electrical field on the cells and whether the shape of the electrical flux (Van der Pol) can change the primary shape of the cells? in which direction can change the shapes? And to try detection and showing the cellular and electrical field changes by an equation similar with gradient. This will indicate the combined geometrical and electrical alterations which is important in terms of their interaction including the excitatory and inhibitory neuronal shape alteration. The morphology and function of neuronal cells play an important role in neuronal network characterization and function [14]. Here we provide an example of shape change by showing the

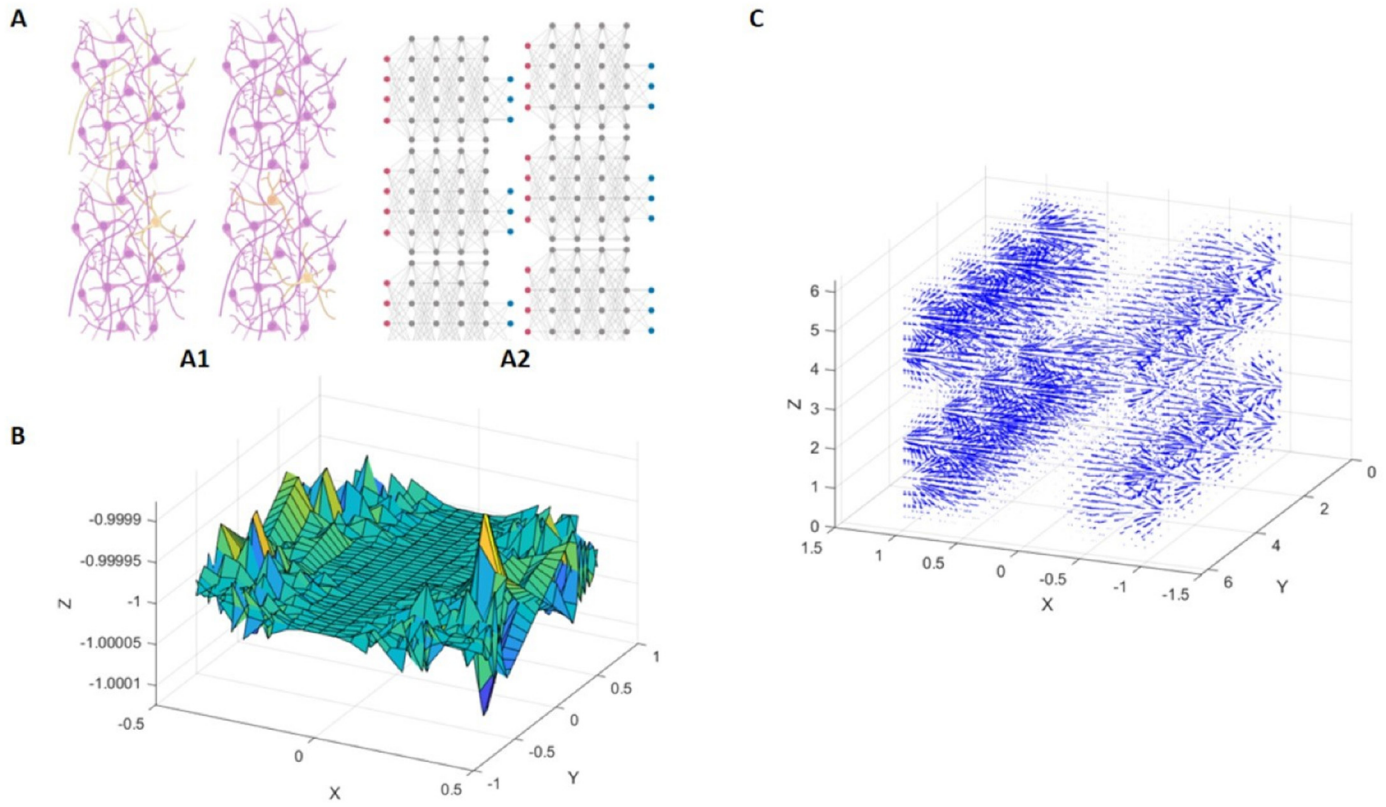

Fig. 7. The plot depicts both schematic illustration (**A**) which shows two ensembles of neurons A1, and its possible connections projected on a plane of the 3D form of neurons, A2, which means 'gradient' in mathematics. Furthermore, the mathematical simulation of the ensemble of neurons is shown in **B**, and its corresponding gradient comes next to it in **C**, which is dense in two sides as a "Vector Field".

Fig. 8.1 that is an illustration of the tensor exterior product of three vectors in three directions on the left and the result is shown on the right in two different 3D shapes depending on their eigenvalues and eigenvectors. Having this notion in mind, we decided to provide a model for our study, so we used the Van der Pol equation [15] and it has been used to show how the neuronal activity is modulated by considering this equation for the purpose of learning process of Non-linear dynamics that evolves the presynaptic and postsynaptic neuronal activity [16]. Van der Pol equation as shown in Fig. 8.2 and its equations below have two phases that are strictly controlled by 'm' value. The similarity of Fig. 8.1 and Fig. 8.2 is that we can produce 3D shape changes using the Van der Pol equation. So, we aimed to simulate different shape change either spherical or pyramidal neuronal cells that generated in this study and explore what happens after applying the Van der Pol equation as described below in formula (22) as equation that plotted as lines in a limit cycle. But the vector field was generated by Van der Pol oscillator, formula (23), (we used 'for formula (22) and 'x' for formula (23) to show the difference), both of the formulas are controlled by 'm' that changes the phase from circle m = 0.1 to non-circle m = 1.

$$y'' - m\left(1-y^2\right)y' + y = 0;$$
$$\text{if } y_1 = y;\ y_2 = y';\ y'' = \left(\frac{dy_2}{dy_1}\right)y_2;\ \frac{dy_2}{dy_1} = k\ldots, \tag{22}$$
$$\boldsymbol{F1} = y_2 = \frac{y_1}{m(1-y_1^2)-k};\ k = \text{Constant}$$

$$x'' - m\left(1-x^2\right)x' + x = 0;\quad \text{if } x_1 = x;\ x_2 = x';\ \left(\frac{dx_1}{dt}\right) = x_2\ldots, \tag{23}$$
$$\boldsymbol{F2} = \left(\frac{dx_2}{dt}\right) = -x_1 - m\left(x_1^2-1\right)x_2;$$

To generate the 'vector field' of Van der Pol oscillation as we have shown in Fig. 8.2, we needed to replace the 'dt' with $r = \sqrt{(d_{x1})^2 + (d_{x2})^2}$, so we rewrote $(\frac{dx_1}{r})$; $(\frac{dx_2}{r})$.

The next step, we needed to explore the effect of Van der Pol on the generated figures in Fig. 6, so we divided them into two groups either spherical or pyramidal and then examined the combined effect. Therefore, we set y_1 respectively equal to formulas of (10), (14), (15), (16). However, to make the neuron more spherical compared to Fig. 6, in order to test the Van der Pol equation; we did change on the 'r' and changed the formulas of (14), (15), (16) into below, as r_2, $(14)_2$, $(15)_2$, $(16)_2$ then we got the following results depicted in Fig. 8.3.1 and Fig. 8.3.2. The variable r_2 is defined by $r = e^{-\cos(p)^2\sin(p)^2}e^{\cos(p)^2+\sin(p)^2}$, $-2\pi < p < 2\pi$, so comes up equations $(\mathbf{14})_2$ to $(\mathbf{16})_2$ as follows:

$$(\mathbf{14})_2 = -r\cos(s)\sin\left(\frac{1}{\text{real}\left(\zeta\left(e^{\frac{r\cos(s)t^5}{120}-\frac{r\cos(s)t^3}{6}+r\cos(s)t}\right)^2\right)}\right)\sin(t)^2$$

$$(\mathbf{15})_2 = -r\sin\left(\frac{1}{\text{real}\left(\zeta\left(e^{\frac{r\sin(s)t^5}{120}-\frac{r\sin(s)t^3}{6}+r\sin(s)t}\right)^2\right)}\right)\sin(s)\sin(t)^2$$

$$(\mathbf{16})_2 = -r\sin\left(\frac{1}{\text{real}\left(\zeta\left(e^{\frac{rt^4}{24}-\frac{rt^2}{2}+r}\right)^2\right)}\right)\cos(t)\sin(t)$$

Furthermore, we calculated the effect of this interaction on the generated 3D manifolds (Spherical or Pyramidal) that is a potentially a differentiable manifold that possess the vector field, so by using the Laplacian vector field (Lvf) that is defined in formula (24). We measured the change of vector field on the generated neurons following applying the Van der Pol oscillator, which depending on the 'm' values they would differ substantially. Then we could find the mean of the difference of Lvf between two phases, before and after applying the Van der Pol oscillator.

$$\nabla^2 f = \nabla(\nabla.f) - \nabla\times(\nabla\times f) \tag{24}$$

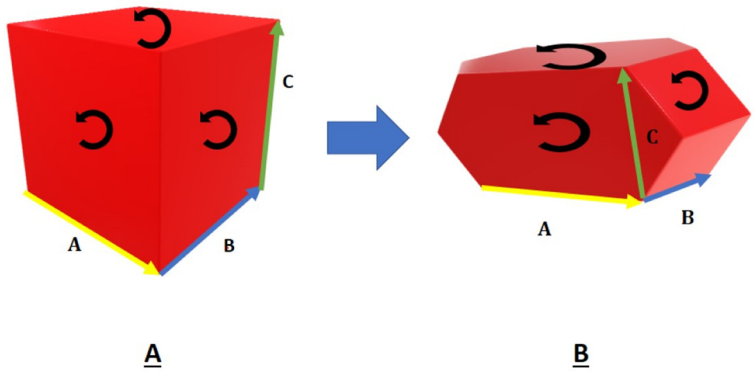

Fig. 8.1. The schematic illustration indicates how an object like a cube can be mathematically transformed into a different shape based on the applied tensor vectors and their exterior product in three directions and their orientation that is the order of their product. Equivalently, we have applied the m=0.1 and M=1 in Fig. 8.2 from Van der Pol equation to transform our 3D shapes. Transforming sphere to a different shape depending on the specific spatial direction (i, j, k) that we apply m or M.

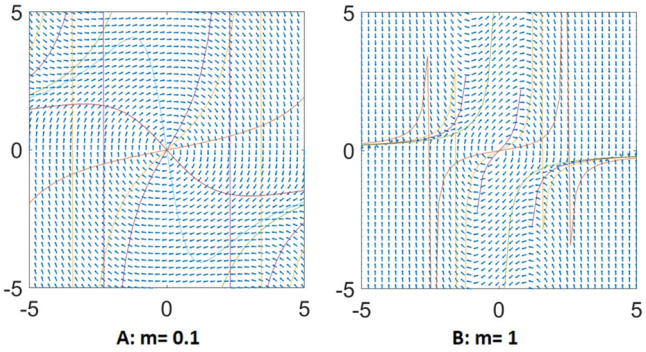

Fig. 8.2. The plots were generated based on Van der Pol equation is explained in more details in the text formula (22) that is to generate the 'Lines' and formula (23) that is to generate the 'vectors', indeed the vector field. As it shown they are different based on the m=0.1 or m=1 values. They differ from circle to non-circle like plot. The values of 'k' have been provided in the codes.

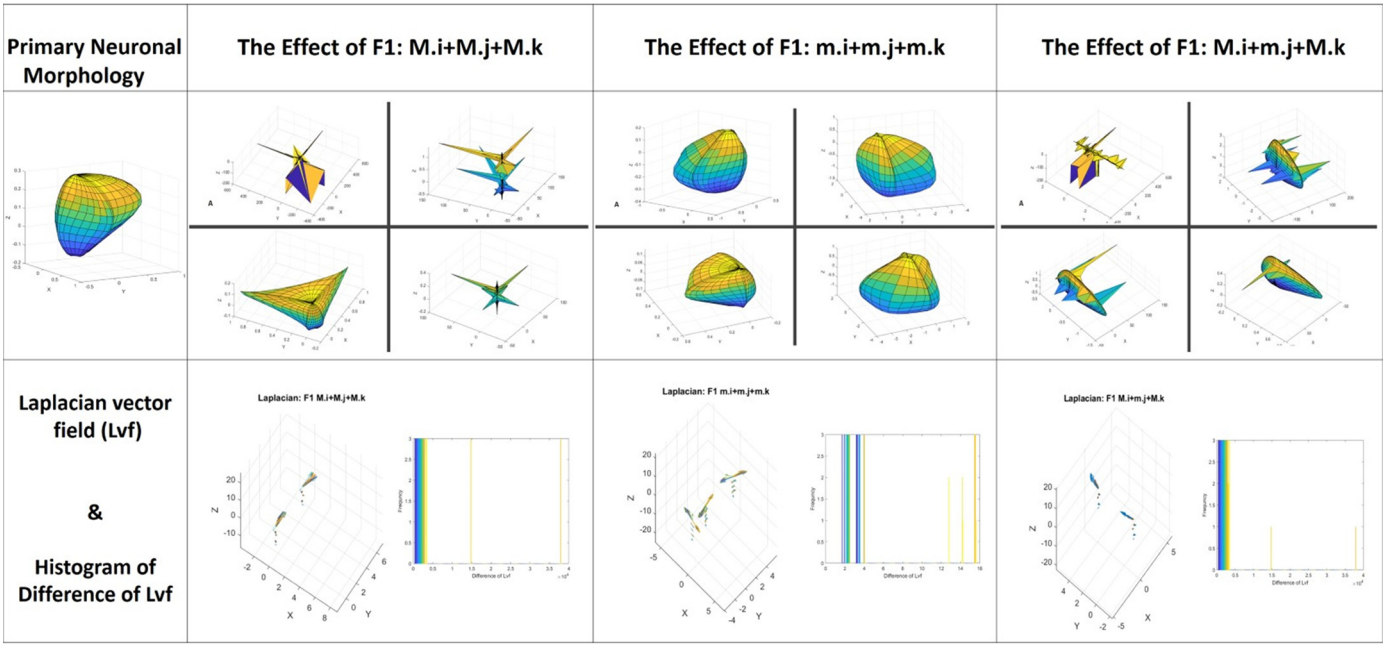

Fig. 8.3.1. We generated the figures based on the Van der Pol and the primary neuronal shape explained in the text. The Primary shape is a pyramid that as an example shows how it differs in the shape as we apply the m=0.1 and M=1 iteration in three directions, (i, j, k), the F1 indicates the formula (22) that was used, so we can see the difference in the shape as we see the (M.i+M.j+M.k) figure makes them more anisotropic while the effect of (m.i+m.j+m.k) is more isotropic that meets our expectations, as one could combine Fig. 8.2, M=1 becomes more anisotropic and m=0.1 becomes more circle and isotropic that has the same effect on the generated plots here. The combination of (M.i+m.j+M.k) is a circular surface (isotropic) along 'y' axis, but anisotropic along two other directions. The Laplacian vector field (Lvf) is also different accordingly and is comparable with the Fig. 8.3.2 as well.

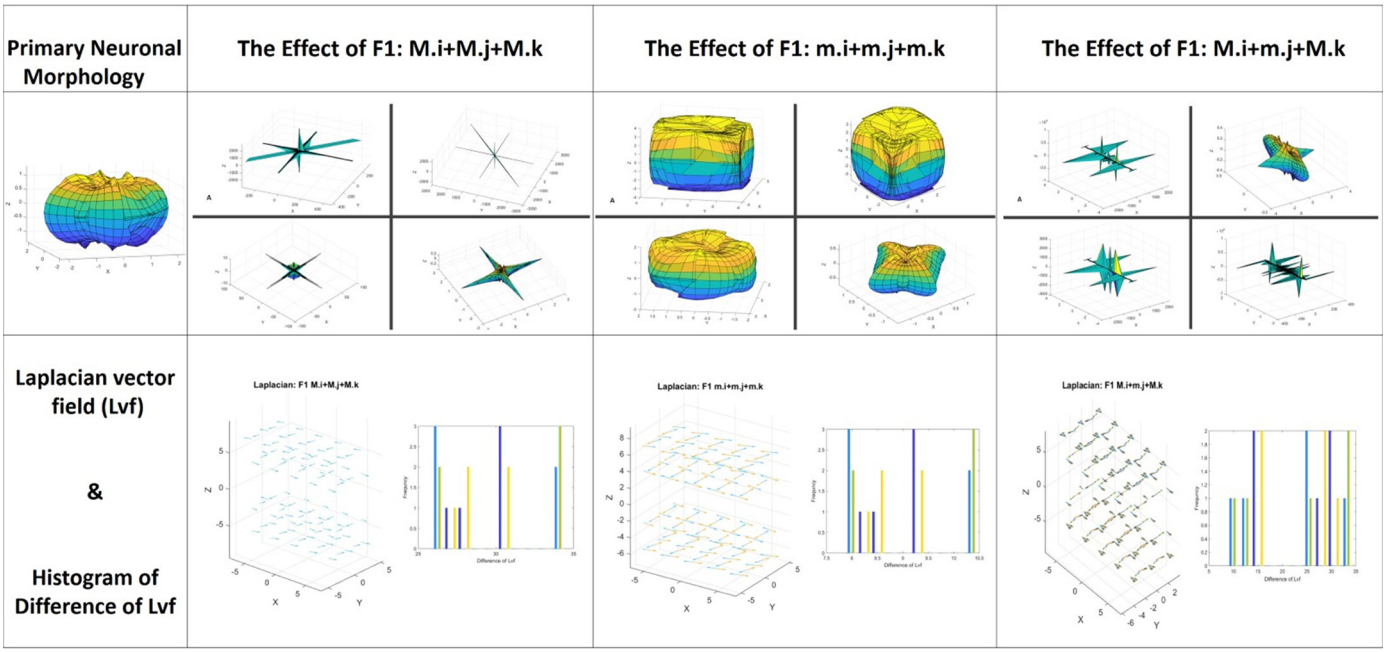

Fig. 8.3.2. Here, it is clearly the anisotropy with M=1 along specified direction and isotropic with m=0.1 in other directions. The Laplacian vector field (Lvf) is more homogeneous but different from Fig. 8.3.1.

Their mean differences considered as an important indicator of how the electrical flux on the cells can affect the cells when is applied in three different directions (i, j, k) with different values of m=0.1 and M=1 at a very short time dt $\approx \varepsilon$. We have $2^3 = 8$ iterations of m and M in three directions (i, j, k) that is shown in Fig. 8.3.1 and Fig. 8.3.2. The iterations list is as followed in three spatial directions: (m.i,m.j,m.k), (M.i,M.j,M.k), (m.i,m.j,M.k), (m.i,M.j,M.k), (M.i,m.j,m.k), (M.i,M.j,m.k), (M.i,m.j,M.k), (m.i,M.j,m.k) that can be applied through either with F1 or F2 formula. This is a real phenomenon that happens between excitatory/inhibitory neurons when electrical flux is spatiotemporally propagated.

The histogram indicates the difference of the mean of Laplacian vector field (Lvf) from the mean difference of Lvf=Lvf (after applying Van der pol) - Lvf (before applying Van der pol), (Fig. 8.3.1 and Fig. 8.3.2). The mean difference of Lvf that is divided into number of 'k' items, is respectively from left to right in Fig. 8.3.1 are 2160, 5, 734, they correspond to the number of M in the equations, so the more anisotropy obtained after applying Van der Pol with M=1 in spatial directions, the higher would be the total mean difference of Lvf, while in spherical shape, the total mean differences of Lvf are respectively from left to right are 29, 9, 22 that are lower compared to the pyramidal form after applying Van der Pol which could indicate a kind of resistance in the spherical manifolds to anisotropic/isotropic vector field change. This phenomenon is interesting as it is equivalent to the inhibitory neurons that are more in spherical shape and excitatory neurons that have more pyramidal shape and here it was shown how the primary geometrical shape can determine the final vector field (anisotropic/isotropic vector field change) after applying Van der Pol oscillator. In our model, neurons have the cellular geometrical features including nucleus structure inside the cells.

2.5. The mathematical model for neuronal organisation and development

Here, we provided a simplified mathematical model that denotes the possible formulation for neuronal organisation which approximated the real neuronal development. The suggested preliminary algorithm addressed neuronal development from different aspects. The schematic illustration of the model is found in Fig. 9.

The definition of the model is:

In formula (27), if 'N' stands for '*Neuronal Organisation and Development Function*' that equals to the '*Curl*' of 'F' where 'F' was a function defined in formula (25) that was followed by known "Curl transformation", see formula (26).

We assumed "F" as the following:

$$F(x,y,z) = F_x(x,y,z)\hat{e}_x + F_y(x,y,z)\hat{e}_y + F_z(x,y,z)\hat{e}_z \tag{25}$$

Then the Curl of the function F is defined as below:

$$C = \nabla \times F = \left(\frac{\partial F_z}{\partial y} - \frac{\partial F_y}{\partial z}\right)\hat{e}_x + \left(\frac{\partial F_x}{\partial z} - \frac{\partial F_z}{\partial x}\right)\hat{e}_y + \left(\frac{\partial F_y}{\partial x} - \frac{\partial F_x}{\partial y}\right)\hat{e}_z \tag{26}$$

The definition of the parameters in formula (27) is shown below as I to IV. Briefly, the parametrisation included the 3D position of cells, in the beginning, cellular position change, shapes and cellular electrical activity.

3D Position of Cells in beginning = $\{\hat{\imath}, \hat{J}, \hat{k}\}$

And we defined the G function and its parameters as:

I. The change in position of cells = $\{dp_1, dp_2, dp_3\}$
II. Shapes = Sphere, ellipsoid, pyramidal approximation, other convex bodies
III. Electrical activity = Excitatory $\{+\}$, Inhibitory $\{-\}$, Excitatory/Inhibitory $\{\pm\}$,
IV. $X(dp_1, s, e_1)$, $Y(dp_2, s, e_2)$, $Z(dp_3, s, e_3)$

$$N = \nabla \times F = \begin{vmatrix} \hat{\imath} & \hat{J} & \hat{k} \\ \frac{\partial}{\partial X} & \frac{\partial}{\partial Y} & \frac{\partial}{\partial Z} \\ G_1(X) & G_2(Y) & G_3(Z) \end{vmatrix} \tag{27}$$

Then the integration was taken, defined by '*Cauchy's integral theorem*', so we defined it as a system in which its spatial position, movement, cell shape and electrical characteristics were ruled by 'Curl' with the assumption of possessing a 'close path' (process) in a 'domain' of the brain so-called 'c' and were connected by "*Cauchy's Integral*" (formula (28)). In general, it met the criteria defined by '*Cauchy's Integral Theorem*'. $f(z)$ was definable in a connected domain containing a close path called 'c'.

Cauchy's Integral: $\oint_C f(z)dz$ (28)

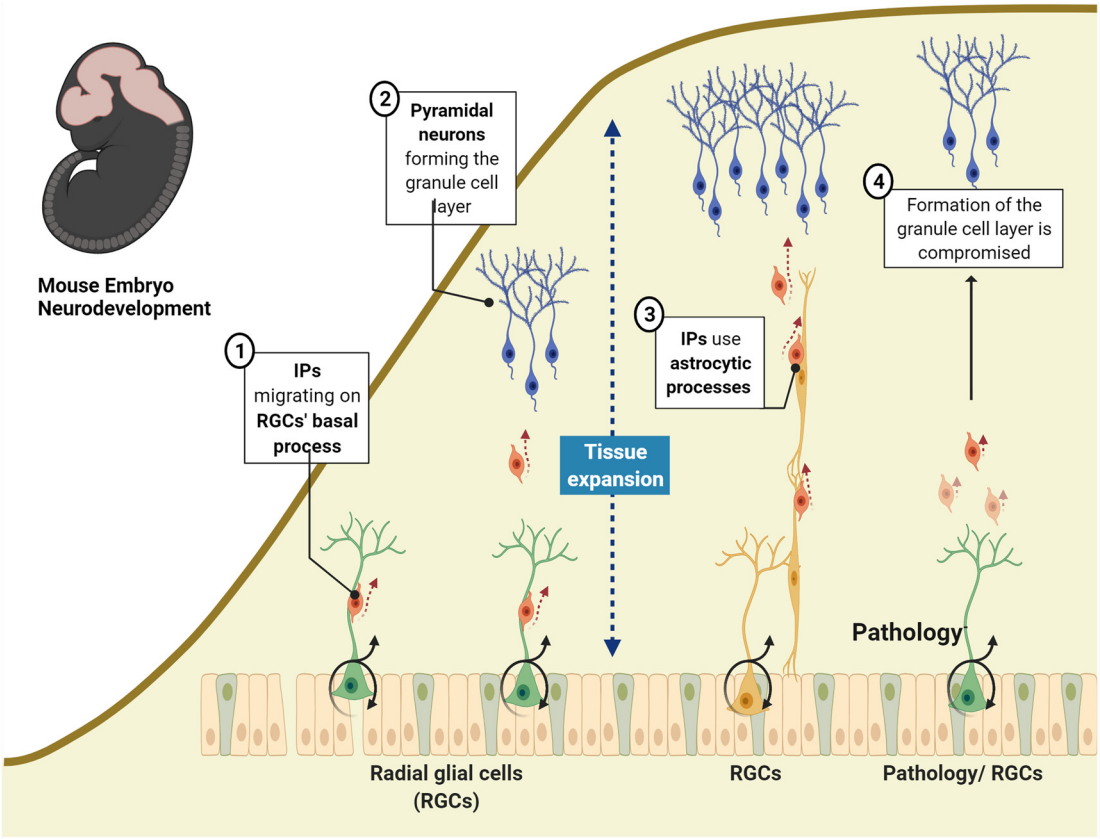

Fig. 9. The schematic illustration (used Biorender.com) shows the neuronal development in the mouse embryo, based on a timeline. We can see the radial glial cells on the left that make a scaffold for the migrating neurons (IPS) while keeping the connections with them from beginning to end. A lack of radial glial cells leads to compromised pathologic cell formation in the "granule cell layer". In our model, we postulate and formularise each step of neuronal development by parametrisation as follows: the coordinates of the primary position (P0) of cells assigned as $\{i, j, k\}$, then a function of variables G(dp,s,e) that include dp, s and e which they stand for dp = change in the position of cells, s = the cell shape and e = the electrical activity.

3. Discussion

This study showed how mathematical modelling [2] may clarify the challenging field of understanding neurodevelopmental processes by considering different aspects of neuronal development including structure, function and networking. For this purpose, neuronal developmental processing was divided into different parts to be quickly addressed and become possible to develop a formulation that approximates the natural neuronal development process. Our modelling suggests that neuronal development occurs in a connected form, between two or more points from the beginning, rather than growing only from one side of the dendrites. As it was shown in our mathematical model, this is important that the spiral, or more complex, pathologic branching occurs when inter-neuronal connections lack adequate cell-cell connections. For example, reelin cells (Cajal) guide neuronal development in cortical layer II-III, therefore when the reelin cells (Cajal) decreases in size or number in those layers within the developmental period, the apical dendrites of pyramidal neurons begin to show hyper-complexity to compensate for reelin cells inadequacy which will be resulted in pathologic neurodevelopment [17]. Hence, it appears that there is a tendency to make the connections for the price of hyper-complexity with "distorted connections", as we verified in this study (Fig. 2 and Fig. 3).

Furthermore, it seems that the 'linear interpolation' is neurobiologically adapted for connectivity from inter-neuronal distance to neurite connections. We showed that neurites orientation follows Lagrangian which minimises the difference of curvatures from a straight-line between two connected points. In another meaning, the curve's orientation tends to be minimal from a straight line. We also used "Taylor expansion" or "Spline" to explain how neurons are connected to each other but we found that these functions are not explanatory enough to describe what would happen if the neurites were not connected from the beginning of neuronal development (data not shown). We verified this issue by applying the "eigenvalues" for the "Surface" and "Line" interactions. In a more exaggerated example, as shown in Fig. 9, due to lack of 'Radial Glial Cells', neuronal migration becomes compromised, then a lack of proper connections with "radial glial cells" at the early stage of neuronal development leads to compromised cortical development. These results implied that adequate connections are obligatory from the beginning of neuronal development to form normal neuronal network [17, 18].

Further, we modelled the neuronal soma (Pyramidal and Non-Pyramidal), including the "Riemann Zeta function", which allowed cells to behave as a neuronal cell that could grow and possess a "mathematically made", "nucleus" which acted as a "Growing Cylindrical Body". This stemmed from the nucleus to the cell surface, the shape changes depending on the" r" value. This was 'Unique' as it stands for continuous cell shape configuration and change in "Shape and Size" simultaneously.

However, we could also have designed this model with the help of "Stokes theorem" that used vector calculus", which meant "Integral of the curl of the vector field" versus the "Riemann Zeta function" of our study to produce the shape of the neurons, or in general, using the "Tensors", that in our previous studies was used to estimate the neuronal size and shape from histological tissues [19, 20]. However, even this mathematical modelling is stationary, it cannot change in a way we explained above from a "nucleus to the outward" with growing possibility, meanwhile our model kept its primary shape (Pyramidal

vs Nonpyramidal), indicating the strength of our mathematical model compared to other formulations used to generate a 3D shape of neurons.

Furthermore, we introduced a mathematically designed neuronal clustering model consisting of two ensembles of well-connected neurons in the form of the 3D plot, resembling neuronal clustering. In the next step, we took the "Gradient", a type of "Partial differential equation of several variables", to explore the neuronal cells' vector fields by using the gradient of the formula that generated the neuronal clustering. This approach disclosed how the underlying vector field depends on the neurons' shape as visualised in Fig. 7. B. This is similar to "Gradient Descent" [21] used in machine learning. We have also shown the effect of Van der Pol oscillator on the shape of change (Anisotropic/Isotropic change) that is equivalent to how electrical flux can change the shape of the cellular vector field based on their primary shape and the quality of the imposed electrical potential. We have analysed the spatial summation of the electrical flux on the neurons, as it is an important biophysical phenomenon [12] equivalently occurring among spherically shaped inhibitory neurons versus excitatory neurons that possess pyramidal morphology. We showed how the primary geometrical shape can be affected by the final vector field depending on the anisotropic versus isotropic vector field change after applying Van der Pol oscillator which explains how neuronal-electrical field interaction works on a biophysical scale that we could show the steps of 3D neuronal alteration.

In the last part of this study, we proposed a formula that tested the hypothesis that neuronal development depends on cell shape, electrical property, and neuronal movement. By taking the Curl of them and meeting Cauchy's Theorem, it could be helpful to provide a model for neuronal clustering and organisation.

4. Conclusion

In this study, we showed how the neuronal development process can be divided into different parts based on the geometrical equivalences and explained how naturally the different parts, including neurites, cell soma, the whole neuronal structure and its vector field are connected. The neuronal-electrical field interaction was explored and simulated in three dimensions to investigate the effect of electrical flux using Van der Pol oscillator on the neuronal shape. The cells could further grow and develop either individually or as an entire system by following the Cauchy's Theorem.

5. Methods

We have used different mathematical formula and algorithms (written in form of functions and function handles) implemented in MATLAB (R2021B) to generate the plots. The Latex of MATLAB was used for the shown formula. The modelling is based on a presumed mouse at developmental age (C57Bl/6J wild-type (WT) mice were purchased from Janvier Labs (Le Genest-Saint-Isle, France) and Charles River Laboratories (Sulzfeld, Germany). They were bred in the animal facility at the University of Gothenburg (Experimental Biomedicine, University of Gothenburg). We show in Fig. 1. A one 3D reconstructed neuron from the hippocampus of a mouse (at the age of Post-natal day 12), as it is easier to conceptualise modelling compared to the human brain, which is more complex.

Declarations

Author contribution statement

Ali H. Rafati: Conceived and designed the experiments; Performed the experiments; Analyzed and interpreted the data; Contributed reagents, materials, analysis tools or data; Wrote the paper.

Maryam Ardalan: Performed the experiments; Contributed reagents, materials, analysis tools or data; Wrote the paper.

Regina T. Vontell: Conceived and designed the experiments; Analyzed and interpreted the data; Wrote the paper.

Carina Mallard, Gregers Wegener: Conceived and designed the experiments; Contributed reagents, materials, analysis tools or data; Wrote the paper.

Funding statement

Maryam Ardalan was supported by Lundbeckfonden (R322-2019-2721), Göteborgs Frimurare Barnhusdirektionen (GLS-975382), Magus Brevalls Stiftelse (2020-03756), Wilhelm och Martina Lundgrens Vetenskapsfond (2021-3808), H.K.H. Kronprinsessan Lovisas Förening för Barnasjukvård (2020-00559) and Stiftelsen Mary von Sydows, född Wijk, donationsfond (2020-1901).

Data availability statement

Data will be made available on request.

Declaration of interests statement

The authors declare no conflict of interest.

Additional information

No additional information is available for this paper.

Acknowledgements

This study was supported by Lundbeck Foundation, Frimurare Barnhusdirektionen, Magus Brevalls Stiftelse, Wilhelm och Martina Lundgrens Vetenskapsfond, Kronprinsessan Lovisas Förening För Barnasjukvård Stiftelsen and Styrelsen för Stiftelsen Mary von Sydows, född Wijk Foundation.

References

[1] O. Sporns, Structure and function of complex brain networks, Dialogues Clin. Neurosci. 15 (3) (2013) 247.
[2] S. Glasauer, M. Dieterich, T. Brandt, Neuronal network-based mathematical modeling of perceived verticality in acute unilateral vestibular lesions: from nerve to thalamus and cortex, J. Neurol. 265 (1) (2018) 101–112.
[3] D. Akarca, et al., A generative network model of neurodevelopment, 2020.
[4] F. Maestú, et al., Neuronal excitation/inhibition imbalance: a core element of a translational perspective on Alzheimer pathophysiology, Ageing Res. Rev. (2021) 101372.
[5] C. Keine, R. Rubsamen, B. Englitz, Inhibition in the auditory brainstem enhances signal representation and regulates gain in complex acoustic environments, eLife 5 (2016).
[6] N.A. Gershenfeld, N. Gershenfeld, The Nature of Mathematical Modeling, Cambridge University Press, 1999.
[7] R.C. O'reilly, Y. Munakata, Computational Explorations in Cognitive Neuroscience: Understanding the Mind by Simulating the Brain, MIT Press, 2000.
[8] S. Fiori, S.-i. Amari, Special issue on "Geometrical methods in neural networks and learning", Neurocomputing 67 (2005) 1–7.
[9] M. Congedo, A. Barachant, R. Bhatia, Riemannian geometry for EEG-based brain-computer interfaces; a primer and a review, Brain-Comput. Interfaces 4 (3) (2017) 155–174.
[10] M. Shafiei, et al., Time delayed chemical synapses and synchronization in multilayer neuronal networks with ephaptic inter-layer coupling, Commun. Nonlinear Sci. Numer. Simul. 84 (2020) 105175.
[11] A. Bahramian, et al., Collective behavior in a two-layer neuronal network with time-varying chemical connections that are controlled by a Petri net, Chaos, Interdiscip. J. Nonlinear Sci. 31 (3) (2021) 033138.
[12] H. Ye, A. Steiger, Neuron matters: electric activation of neuronal tissue is dependent on the interaction between the neuron and the electric field, J. NeuroEng. Rehabil. 12 (2015) 65.
[13] A. Kovacs, et al., Magnetostatics and micromagnetics with physics informed neural networks, J. Magn. Magn. Mater. (2022) 168951.
[14] E. Meijering, Neuron tracing in perspective, Cytometry, Part A 77 (7) (2010) 693–704.
[15] van der Pol Oscillator, in: Essentials of Mathematica: With Applications to Mathematics and Physics, Springer New York, New York, NY, 2007, pp. 505–508.

[16] A. Gilra, W. Gerstner, Predicting non-linear dynamics by stable local learning in a recurrent spiking neural network, eLife 6 (2017) e28295.
[17] P. Chameau, et al., The N-terminal region of reelin regulates postnatal dendritic maturation of cortical pyramidal neurons, Proc. Natl. Acad. Sci 106 (17) (2009) 7227–7232.
[18] T.J. Nowakowski, et al., Loss of functional Dicer in mouse radial glia cell-autonomously prolongs cortical neurogenesis, Dev. Biol. 382 (2) (2013) 530–537.
[19] A.H. Rafati, et al., Estimation of shape and orientation of neurons in thick histological sections by volume tensors, Acta Stereol. (2015).
[20] A.H. Rafati, et al., Stereological estimation of particle shape and orientation from volume tensors, J. Microsc. 263 (3) (2016) 229–237.
[21] M. Zinkevich, et al., Parallelized stochastic gradient descent, in: NIPS, Citeseer, 2010.